ANTIOXIDANTS & REDOX SIGNALING
Volume 14, Number 11, 2011

DOI: 10.1089/ars.2009.3059

ORIGINAL RESEARCH COMMUNICATION

DJ-1 Cleavage by Matrix Metalloproteinase 3 Mediates Oxidative Stress-Induced Dopaminergic Cell Death

Dong-Hee Choi,[1,2] Onyou Hwang,[3] Kyoung-Hee Lee,[2] Jongmin Lee,[2]
M. Flint Beal,[1] and Yoon-Seong Kim[1,4]

Abstract

Oxidative stress is commonly implicated in aging and neurodegenerative conditions such as Parkinson's disease (PD). Mutations in DJ-1 are associated with autosomal recessive early-onset PD. We investigated whether DJ-1 can be degraded in oxidative-stressed dopaminergic neuronal cells, leading to loss of its protective role against oxidative stress. We have shown previously and herein that the active form of matrix metalloproteinase-3 (MMP3) was accumulated in dopamine-producing CATH.a cells in the presence of MPP^+. We show that catalytically active MMP3 cleaved DJ-1, and impaired its antioxidant function. In CATH.a cells, both monomeric and dimeric forms of DJ-1 were diminished in the presence of MPP^+, and this was reversed by MMP3 knockdown or inhibition. While DJ-1 expression was decreased in the substantia nigra of mice administered with MPTP, its degradation was largely attenuated in *MMP3* knockout mice. The AKT-signaling pathway, thought to mediate the effect of DJ-1 on cell survival, was also altered. MPP^+ caused decrease in both phospho-Thr308 and phospho-Ser473 forms of AKT, and this was restored by NNGH. Our data suggest that DJ-1 is fragmented by the intracellular MMP3 in response to cell stress, abolishing the protective role of DJ-1 against oxidative damage, and this contributes to the pathogenesis of PD. *Antioxid. Redox Signal.* 14, 2137–2150.

Introduction

Parkinson's disease (PD) is an age-related and progressive neurodegenerative movement disorder caused by the selective loss of dopamine (DA)-producing neurons in the substantia nigra (SN) pars compacta. Cellular stresses derived from oxidative stress, mitochondrial dysfunction, inflammation, and impairment of the protein degradation system have all shown to lead to death of DA cells (11, 17, 25).

While the majority of PD cases is idiopathic, genetic factors also contribute to the pathogenesis. Mutations in *DJ-1* in the PARK7 locus are associated with autosomal recessive early-onset PD, which accounts for 1%–2% of all early onset PD cases (6). *DJ-1* encodes a 189 amino acid protein that is a member of the ThiJ/PfPI superfamily (16, 33, 37). DJ-1 is expressed in both neurons and astrocytes in the brain (5, 11, 37), as well as in various other organs (37). At the subcellular level, it is found in the matrix and the intermembrane space of the mitochondria (3), as well as in the cytosol (4). DJ-1 works as an atypical peroxiredoxin-like peroxidase that scavenges H_2O_2 (3, 7), and studies have shown that DJ-1 can provide protection against oxidative, proteasomal, and mitochondrial stresses (37), and that loss of its function is associated with the onset of PD (3). DJ-1 has three cysteine residues at amino acids 46, 53, and 106 (C46, C53, and C106, respectively) (36). Of the three cysteine residues, C106 is oxidized to sulfinic acid during the peroxidase reaction and is therefore necessary for DJ-1 to be functionally active (7, 36). DJ-1 becomes inactive if C106 is superfluously oxidized, and such oxidized DJ-1 has been observed in patients with idiopathic PD (36). DJ-1 knockout (KO) mice show a deficit in scavenging mitochondrial H_2O_2 (3, 7), and this H_2O_2 scavenging activity is a prerequisite for cell protection against H_2O_2-induced death and ischemia-induced damage (2, 43). Another irreversibly oxidized form of DJ-1, produced by carbonylation and methionine oxidation (9), has also been found in PD cases. In addition, DJ-1 has been reported to modulate the PTEN/AKT survival pathway (22, 48) and disrupt the Ask1-mediated apoptotic signaling (19). All these findings point to the importance of intact DJ-1 in protection of dopaminergic (DArgic) neurons against oxidative stress.

We have previously demonstrated that the active form of matrix metalloproteinase 3 (MMP3) can be generated intracellularly in response to cell stress and is involved in apoptosis

[1]Neurology/Neuroscience Department, Weill Medical College of Cornell University, New York, New York.
[2]Center for Geriatric Neuroscience Research, Institute of Biomedical Science and Technology, Konkuk University, Seoul, Korea.
[3]Department of Biochemistry and Molecular Biology, University of Ulsan College of Medicine, Seoul, Korea.
[4]College of Nursing Science, Kyunghee University, Seoul, South Korea.

of DArgic cells (8). This suggested the possibility that there might be some target proteins that are cleaved by this endoprotease inside the cell. Indeed, α-synuclein has been shown to be cleaved by MMP3 and that the fragmented α-synuclein is more prone to aggregation and rendering toxicity (26, 40). In fact, our previous study showed that 1-methyl-4-phenyl-1,2,3,6 tetrahydropyridine (MPTP)-elicited degeneration of nigrostriatal DA neurons is largely attenuated in *MMP3* KO mice (23). Based on these observations, we hypothesized that DJ-1 may be cleaved by MMP3 and that this renders the cells more vulnerable. In the present study, we sought to investigate whether MMP3 directly cleaves DJ-1, and that the cleavage abolishes its antioxidant activity against H_2O_2, interferes with the AKT survival pathway, and increases the sensitivity of DArgic cells to cellular stress.

Materials and Methods

Materials

Fetal bovine serum (FBS), horse serum, RPMI 1640, trypsin/EDTA, and penicillin-streptomycin were purchased from GibcoBRL (Gaithersburg, MD). N-isobutyl-N-(4-methoxyphenylsulfonyl) glycyl hydroxamic acid (NNGH) and MMP3 fluorescent assay kit were purchased from BIOMOL International, L.P. (Plymouth Meeting, PA). The recombinant catalytic domain of MMP3 protein was from Calbiochem (San Diego, CA). Antibodies used are as follows: Goat polyclonal anti-MMP3 (R&D systems, Minneapolis, MN), goat polyclonal anti-DJ-1, rabbit polyclonal anti-DJ-1, and mouse monoclonal anti-SOD2 (Santa-Cruz Biotechnology, Santa Cruz, CA), mouse monoclonal anti-TH antibody (Sigma-Aldrich St. Louis, MO), mouse monoclonal anti-DJ-1 (Stressgen, Ann Arbor, MI), rabbit anti-phospho-Akt polyclonal antibodies (phospho-Ser473 and phosphor-Thr308) (Cell Signaling, Beverly, MA), mouse monoclonal anti-Flag antibody (Sigma-Aldrich) and mouse monoclonal anti-V5 antibody (Invitrogen, Carlsbad, CA). NuPAGE Tris-glycine ready gels (4%∼12% polyacrylamide), prestained SDS-PAGE standards (broad range), Trizol reagent, and Amplex red kits were from Invitrogen. The bacterial (*E. coli*) host and the cloning vector pET-30 Ek/LIC (which contains the nucleotide sequence coding for six histidines) were obtained from Novagen (Madison, WI). Primers were synthesized at Invitrogen, and Taq polymerase, nucleotides, and Fugene6 were purchased form Roche Applied Science (Indianapolis, IN). Gel extraction kit, and Ni-NTA Superflow column matrix were obtained from QIAGEN (Valencia, CA). CelLyticB Bacterial Cell Lysis/Extraction Reagent, Luria Bertani (LB) broth, isopropyl β-thiogalactopyranoside (IPTG), kanamycin, SDS, DTT, EDTA, imidazole were obtained from Sigma-Aldrich. All other chemicals were reagent grade and were from Sigma-Aldrich or Merck (Rahway, NJ).

Animals and MPTP injection and immunohistochemistry

All procedures were approved by the Animal Experiment Review Board of Laboratory Animal Research Center of Konkuk University. *MMP-3* knockout (KO) mice (C57BL/6x129SvEv), originally developed by Mudgett *et al.* (28), and their wild-type (WT) animals were obtained from Taconic Farms (Germantown, NY) and bred at the specific pathogen-free animal facility of Asan Institute for Life Science, University of Ulsan of College Medicine (Seoul, Korea). WT and *MMP-3* null mice (8 weeks, body weight 20 + 2 g) received 4 intraperitoneal (i.p.) injections of PBS or MPTP (4×15 mg/kg at 2 h intervals) and were sacrificed after 7 days (5 mice per group). Immunohistochemistry was performed using the protocol described previously (23). Briefly, mice were deeply anesthetized with sodium pentobarbital (120 mg/kg) and transcardially perfused with saline containing 0.5% sodium nitrite and 10 U/ml heparin sulfate, followed by cold 4% formaldehyde generated from paraformaldehyde in 0.1*M* PBS (pH 7.2). Brains were postfixed in the same solution for 1 h and infiltrated with 30% sucrose overnight. Free-floating sections (30 μm) were obtained from the striata and SN using a cryocut microtome (CM1850, Leica, Wetzlar, Germany). Sections were washed in 0.1 *M* PBS, incubated in 0.1 *M* PBS containing 5% normal horse serum and 0.3% TritonX-100 for 1 h, and subsequently incubated overnight with both TH (1:1000) and DJ-1 (1:500) antibodies at 4°C. The sections were then incubated with Alexa Flour 488 conjugated—and Alexa Flour 546 conjugated—secondary IgG (1:200) for 1 h in a humidified chamber. PBS (0.1 *M*, pH 7.4) containing 1.5% normal horse serum was used to wash sections on slides between all steps. The sections were washed in PBS, mounted on a glass slide, and viewed by confocal microscopy (FV-1000 spectral, Olympus, PA).

Expression of N-terminal Flag-tagged and C-terminal V5-tagged human DJ-1 in COS cells

pcDNA3.0 DJ-1-V5 plasmid DNA, kindly provided by Dr. Jin H. Son, was used to express C-terminal V5-tagged human DJ-1 (CT-V5-DJ-1). For construction of the N-terminal Flag-tagged and C-terminal V5-tagged plasmid DNA (Flag-DJ-1-V5), PCR was performed using the CT-V5-DJ-1 plasmid DNA as a template. The PCR product was cloned into the p3xFLAG-Myc-CMV™-25 expression Vector (Sigma-Aldrich). COS cells were plated on a 100 mm dish at a density of 5×10^6 cells one day prior to transfection. 15 μl of Fugene6 reagent was diluted directly into 500 μl of OPTI-MEM and incubated at room temperature for 5–10 min before the diluted reagent was added to the plasmid DNA in polystyrene tubes. The DNA–Fugene6 mixture was then incubated at room temperature for an additional 15–20 min to allow complex formation. The DNA–Fugene6 complex was added onto the COS cells. The cells were incubated for 48 h in the presence of the transfection mixture before analysis. Flag-DJ-1-V5 was used only for the *in vitro* test for cleavage of DJ-1 by cMMP3.

Generation of recombinant human DJ-1 peptides in E.coli

For construction of the full-length human DJ-1, polymerase chain reaction (PCR) was performed using the above-mentioned plasmid DNA (CT-V5-DJ-1) as a template. The PCR product was cloned into the pET-30 Ek/LIC expression vector. His-tagged recombinant human DJ-1 was produced in BL21 *E. coli* cells induced with 1 m*M* IPTG for 4 h at 37°C. Bacterial pellets were resuspended in 50 m*M* sodium phosphate (pH 6.8) and 300 m*M* sodium chloride, and lysed by sonication. Lysates were cleared by centrifugation at 20,000 *g* for 20 min, and the supernatant was incubated with NTA-Ni-conjugated agarose resin for 1 h at 4°C. The resin was

subsequently washed five times with 20 resin volumes of lysis buffer containing 20 m*M* imidazole, and protein was eluted in five fractions with two resin volumes of lysis buffer containing 250 m*M* imidazole. Recombinant protein elutions were confirmed to be of 99% purity by SDS- PAGE and colloidal Coomassie staining.

Cleavage of DJ-1 by cMMP3

The lysate of COS cells transiently transfected with Flag-DJ-1-V5 and was incubated with 50, 100, or 200 ng/ml of cMMP3 or 200 ng/ml active MMP-9 in the absence or presence of 1 μM NNGH for 2 h at 37°C. The samples were then loaded in total onto each lane of SDS-PAGE for Western blot analysis against Flag or V5. For the elimination of H_2O_2, 10 μg/ml recombinant and purified human DJ-1 protein was incubated with 100 ng/ml cMMP3 in the presence of 20 m*M* Tris-HCl, pH 7.2, 150 m*M* NaCl, 1 m*M* $CaCl_2$ at 37°C for 2 h. To assess the ability of cMMP3 to cleave DJ-1 protein directly, DJ-1 was incubated in the above-mentioned buffer with NNGH or active MMP-9. After the digestion, the solutions were used for H_2O_2 detection using an Amplex Red kit.

Digestion of rDJ-1 by cMMP3 and nano-liquid chromatography–mass spectrometry/mass spectrometry analysis

500 ng of recombinant DJ-1 (rDJ-1) was incubated with 0.5 μg of recombinant catalytic domain of human MMP3 (cMMP3) in 20 μl PBS for overnight at 37°C. The digested peptides were extracted twice with 5% formic acid in 50% acetonitrile solution at room temperature for 20 min and desalted using C18 ZipTips (Millipore, Billerica, MA) before mass spectrometry (MS) analysis. The desalted peptides were loaded onto a fused silica microcapillary column (12 cm× 75 μm) packed with the C18 reversed phase resin (5 μm, 200 Å). Liquid chromatography separation was conducted under a linear gradient as follows: a 3%–40% solvent B (0.1% formic acid in 100% ACN) gradient, with a flow rate of 250 nl/min, for 60 min. The column was directly connected to a LTQ linear ion-trap mass spectrometer (ThermoFinnigan, San Jose, CA) equipped with a nano-electrospray ion source. The electrospray voltage was set at 2.05 kV, and the threshold for switching from MS to MS/MS was 500. The normalized collision energy for MS/MS was 35% of main radio frequency amplitude (RF) and the duration of activation was 30 ms. All spectra were acquired in data-dependent scan mode. Each full MS scan was followed by five MS/MS scans corresponding from the most intense to the fifth intense peaks of full MS scan. Repeat count of peak for dynamic exclusion was 1, and its repeat duration was 30 s. The dynamic exclusion duration was set for 180 s and width of exclusion mass was ± 1.5 Da. The list size of dynamic exclusion was 50. The collected MS/MS spectra were searched using SEQUEST (ThermoFinnigan) program with the selected criteria of the oxidation on Met (+16 Da), Carboxyamidomethylation on Cys (+57 Da) as variable modifications.

Detection of H_2O_2 by Amplex Red assay

Polystyrene tubes containing 0.5 ml of the working solution and either 0.5 ml of the various H_2O_2 calibration standards or 0.5 ml aliquots of the samples were incubated for 30 min at room temperature. The samples were transferred into 96-well plates and fluorescence was measured with a spectrofluorometer (FluoroMax-3, Jobin Yvon, NJ) using excitation at 530 ± 2 nm and fluorescence detection at 585 ± 2 nm.

Cell cultures

CATH.a cells were grown in RPMI 1640 containing 8% horse serum, 4% FBS, and COS cells in DMEM containing 10% FBS. The cells were maintained in the above medium containing 100 IU/l penicillin and 10 μg/ml streptomycin at 37°C in 95% air and 5% CO_2 in humidified atmosphere. For experiments, the cells were plated on polystyrene tissue culture dishes at a density of 5×10^4 cells/well in 96-well culture plates, $1.5\sim3\times10^5$ cells/well in 24 well culture plates, 1.5×10^6 cells/well in 6-well culture plates. After 24 h, the cells were fed with fresh medium and treated with MPP^+ and/or other drugs.

MMP3 activity assay

MMP3 activity was measured following the manufacturer's instructions. To measure the activity of intracellular MMP3, cells were washed in PBS and lysed by brief sonication in the assay buffer (50 m*M* MES, 10 m*M* $CaCl_2$, and 0.05% Brij-35, pH 6.0). 50 μg of the cell lysate protein was transferred to 96 wells, to which the assay buffer was added to a total volume of 199 μl. After incubation for 1 h at 37°C, reaction was started by adding 1 μl (4 μM final concentration) of substrate (Mca-Pro- Leu-Gly-Leu-Dpa-Ala-Arg-NH_2). The plates were read continuously in a fluorescence microplate reader (Molecular Devices, Menlo Park, CA) over 30 min (excitation at 328 nm/emission at 393 nm) and the rate of product formation was determined from the linear range.

Assay of the cellular ROS contents

Cells were incubated with 2′,7′-dichlorodihydrofluorescein diacetate (DCFDA; 100 μM in DMSO; Invitrogen, Carlsbad, CA) for 1 h at 37°C, and then washed twice with PBS. The cellular free radical content was assayed by measuring the 2′,7′-dichlorofluorescein fluorescence by using a microplate reader (excitation at 485 nm/emission at 535 nm).

Cell staining

Cells grown and treated on a cover slide were fixed in cold 4% paraformaldehyde in 0.1 *M* phosphate-buffered saline (PBS), pH 7.4 for 30 min at room temperature. After washing twice in PBS, the cells were incubated for 1 h in blocking solution (5% BSA and 0.3% Triton X-100 in 0.1 *M* PBS). The cells were then incubated overnight with appropriate primary antibody (MMP3, 1:500; DJ-1, 1:500; SOD2, 1:100) diluted in incubation solution (2% BSA and 0.2% Triton X-100 in 0.1 *M* PBS) at 4°C and washed twice in PBS. The samples were incubated at 24°C for 1 h with appropriate fluorescence-labeled secondary antibody (Alexa Fluor 546 conjugated donkey anti-goat IgG; Cy5 conjugated donkey anti-rabbit IgG; Alexa Fluor 488 conjugated donkey anti-mouse IgG) diluted 1:200 in the incubation solution. As a negative control, the samples were incubated with the respective secondary antibodies only. The cells were washed in PBS, mounted on a glass slide, and viewed by confocal microscopy (FV-1000 spectral, Olympus, Center Valley, PA).

Cytoplasmic and mitochondrial fractionation

Cytosolic and mitochondrial extracts were prepared from CATH.a cells in the absence or presence of MPP^+. The cells were washed with ice-cold phosphate-buffered saline and incubated in buffer A (10 m*M* Tris HCl [pH 7.5], 2 m*M* $MgCl_2$, 3 m*M* CaCl, 300 m*M* sucrose, 0.1 m*M* dithiothreitol, protease inhibitor cocktail contains 4-(2-Aminoethyl) benzenesulfonyl fluoride (AEBSF), pepstatin A, bestatin, leupeptin, aprotinin, and trans-epoxysuccinyl-L-leucyl-amido(4-guanidino)-butane(E64)) on ice for 15 min. After incubation, 10% IGEPAL CA-630 solution added to a final concentration of 0.6%. After centrifugation (10,000 *g*, 30 sec), the supernatants were transferred to a fresh tube. This fraction was the cytoplasmic fraction. For mitochondrial fractionation, the cells were washed with ice-cold phosphate-buffered saline and homogenate in buffer B (225 m*M* mannitol, 75 m*M* sucrose, 5 m*M* HEPES, 1 m*M* EGTA, and 0.1 mg/ml BSA) with glass homogenizer. After centrifugation (6000 rpm, 5 min, at 4°C), the supernatants were transferred to a fresh tube. After centrifugation at 14,000 rpm for 12 min at 4°C, the pellet (crude mitochondrial fraction) was resuspended with 1 ml of 12% percoll and resuspension was put on 9 ml of 23% percoll in buffer B without BSA. After centrifugation at 25,000 rpm for 16 min at 4°C, the middle layer (pure mitochondrial fraction) was transferred to a fresh tube and washed with buffer containing 225 m*M* mannitol, 75 m*M* sucrose 5 m*M* HEPES. After centrifugation at 14,000 rpm for 11 min at 4°C, aliquots of mitochondrial extract protein were frozen at −70°C. For the determination of purity, 15 μg of soluble protein per lane was subjected to SDS-PAGE and electrotransferred onto PVDF membrane. Specific protein bands were detected by using specific anti-Akt antibody as a marker cytoplasmic fraction or anti-Tim23 antibody as a marker mitochondrial fraction and Enhanced Chemiluminescence.

Western blot analysis

Cells were washed with ice-cold PBS and lysed on ice in RIPA buffer (50 m*M* Tris-HCl pH 7.4, 150 m*M* NaCl. 1% NP40, 0.25% Na-deoxycholate, and 0.1% SDS) containing protease inhibitor mixture and phosphatase inhibitors (Sigma-Aldrich). To detect DJ-1 dimers, confluent cells were washed twice with PBS containing 1 m*M* $MgCl_2$ and 1 m*M* $CaCl_2$. One m*M* of the chemical crosslinker disuccinimidyl suberate (DSS) was added directly to the cells. After the cells were incubated for 30 min at room temperature, the cells were washed twice with PBS followed by PBS containing 50 m*M* Tris–HCl (pH 7.4) (5). 30 μg of soluble protein was subjected to SDS-PAGE and electrotransferred onto PVDF membrane. Specific protein bands were detected by using specific antibodies (anti-MMP3, 1:1000; anti-DJ-1, 1:1000; anti-flag, 1:4000; anti V5 1:5000) and anti-phospho-AKT (Ser473 and Thr308, 1:500; anti-V5, 1:5000) and enhanced chemiluminescence. For co-immunoprecipitaion (IP) followed by Western blot analysis, 300 μg of cytosolic fractions was incubated with goat anti-MMP3 antibody in combination with protein A/G agarose beads overnight in a cold room. After spinning down, the pellet was washed with RIPA buffer three times. After washing, IP pellet was subjected to SDS-PAGE and electrotransferred onto PVDF membrane. DJ-1 was detected by Western blot analysis.

Total RNA extraction and RT-PCR analysis

Total RNA was extracted from CATH.a cells using Trizol reagent. Reverse transcription was performed for 1 h at 42°C with 1 μg of total RNA using 20 unit/μl of AMV reverse transcriptase (Roche Applied Science, Basel, Switzerland), and oligo-p(dT)15 as a primer. The samples were then heated at 99°C for 5 min to terminate the reaction. The cDNA obtained from 0.1 μg total RNA was used as a template for PCR amplification. Oligonucleotide primers were designed based on Genebank entries for mouse DJ-1 (sense, 5′-GCTT CCAA AAGAGCTCTGGTCA-3′; antisense, 5′- GCTCTAGTCTTTG AGAACAAGC-3′) and rat GAPDH (sense, 5′- ATCACCATC TTCCAGGAGCG-3′; antisense, 5′- GATGGCATGGACTGT GGTCA-3′). PCR mixes contained 10 μl of 2X PCR buffer, 1.25 m*M* of each dNTP, 100 p*M* of each forward and reverse primer, and 2.5 units of Taq polymerase in the final volume of 20 μl. Amplification was performed in 30 cycles at 58°C, 30 sec; 72°C, 1 min; and 94°C, 30 sec. After the last cycle, all samples were incubated for an additional 10 min at 72°C. PCR fragments were analyzed on 1.5% agarose gel in 0.5XTBE containing ethidium bromide. Amplification of GAPDH, a relatively invariant internal reference RNA, was performed in parallel, and cDNA amounts were normalized against GAPDH mRNA levels. The primer set specifically recognized only the gene of interest as indicated by amplification of a single band of expected size. Real-time PCR was performed using the ABI prism 7900 HT sequence detection system (Applied Biosystems, Foster City, CA) based on the 5′-nuclease assay for DJ-1 gene and housekeeping gene GAPDH. Relative expression was calculated using the ΔΔ Ct method (27).

Preparation and transfection of siRNA

Sense and anti-sense oligonucleotides corresponding to the mouse MMP3 cDNA sequences were used: AAUUCCAAC UGCGAAGAUCCACUGA (#1), UUAAUCCCUGGUCCAG GUGCAUAGG (#2), and AUACCAUCUACAUCAUCUUG AGAGA (#3). Double-stranded siRNAs were synthesized chemically and modified into stealth siRNA to enhance the stability *in vitro*. The stealth siRNA with a similar GC content as MMP3 stealth siRNA was used as negative control. When CATH.a cell cultures reached approximately 80% confluency, Lipofectamin™ 2000 and siRNAs (final concentration 33 n*M*) were added. After 6 h incubation, the culture medium was changed and cells were maintained for additional 30 h before MPP^+ treatment.

Lactate dehydrogenase assay

Degrees of cell death were assessed by activity of lactate dehydrogenase (LDH) released into the culture medium using the cytotoxic assay kit (Promega Bioscience, San Luis Obispo, CA). Aliquots (50 μl) of cell culture medium were incubated with 50 μl of LDH substrates for 15 ~ 30 min at room temperature, followed by the addition of 50 μl stop solution (0.1% acetic acid). Absorbance at 490 nm was measured using a microplate spectrophotometer (Spectra Max 340 pc; Molecular Devices).

Statistical analysis

Experimental data represent mean ± S.E. of experiments repeated 4 to 6 times. Comparisons were made using ANOVA

and Newman–Keuls multiple comparisons test. $P < 0.05$ was considered statistically significant for all analyses.

Results

Increases in ROS level and MMP3 activity in MPP$^+$-treated CATH.a cells

We first tested whether ROS level and MMP3 activity might be altered by MPP$^+$, a toxic metabolite of MPTP, in CATH.a cells, a DA-producing neuronal cell line (41) extensively used to study the DArgic cell death induced by oxidative stress (8, 30). The level of ROS was increased in a dose-dependent manner from 100 to 300 μM of MPP$^+$ in 1 to 6 h (Fig. 1A), and MMP3 activity was similarly increased in 24 h (Fig. 1B). Consistent with our previous observation that actMMP3 can be produced inside DArgic cells under cellular stress (8), we demonstrated that intracellular MMP3 activity was increased also by MPP$^+$ and that this is accompanied by elevation of ROS generation.

Attenuation of MPP$^+$-mediated ROS generation by inhibition of MMP3 activity or expression

It was also tested whether MMP3 plays a role in the MPP$^+$-mediated ROS generation. CATH.a cells were pretreated with 30 μM of NNGH, a MMP3 inhibitor, for 1 h, followed by 300 μM MPP$^+$ for 6 h. The MPP$^+$-induced ROS generation was significantly attenuated in presence of NNGH (from 156.00 ± 12.00% to 130.00 + 3.70%) (Fig. 2A). For further verification, small interference RNA (siRNA)-mediated MMP3 knockdown was employed. Among the three different MMP3 siRNA sequences (#1 ~ #3) tested, the third one showed maximal knockdown efficiency, as verified by RT-PCR and Western blot analysis (Figs. 2C and 2D). Both the pro- and active form of MMP3 protein were significantly attenuated (from 2.53-fold to 1.38-fold and from 2.99-fold to 1.50-fold, respectively) (Fig. 2D). This MMP3 siRNA sequence was used to investigate whether the knockdown might prevent the MPP$^+$-induced ROS generation. Compared to the cells transfected with negative control siRNA (152.34 + 10.57%), the MMP-3 knockdown significantly reduced the ROS generation to 127.48 + 8.74% (Fig. 2B).

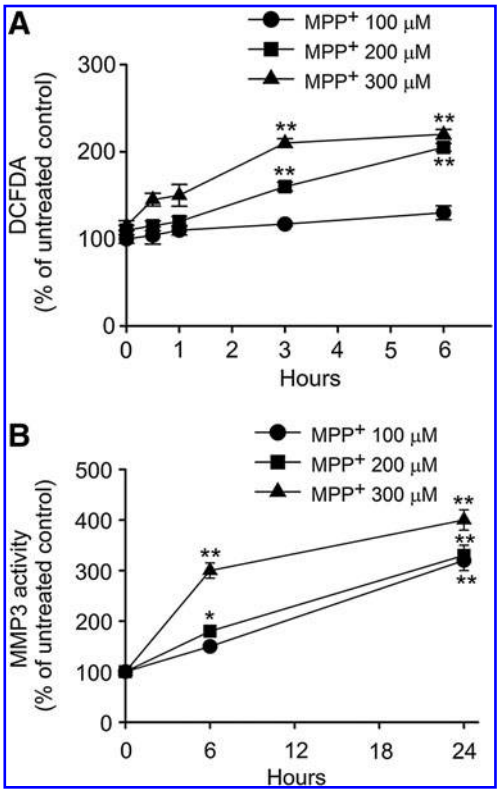

FIG. 1. ROS level and MMP3 activity are increased in CATH.a cells exposed to MPP$^+$. (A) ROS levels in CATH.a cells were measured using DCFDA at 0.5, 1, 3, and 6 h after MPP$^+$ (100, 200, and 300 μM) treatment. **(B)** MMP3 activity was measured in CATH.a cell lysates at 6 h and 24 h after MPP$^+$ (100, 200, and 300 μM) treatment; *$p < 0.05$, **$p < 0.01$ vs. time zero.

Accumulation of the active form of MMP3 and degradation of DJ-1 in MPP$^+$-stressed CATH.a cells

We investigated whether this increase in MMP3 activity might accompany a change in DJ-1. Expressions of both the pro- (proMMP3; 55 kD) and active form (actMMP3; 48 kD) were elevated in CATH.a cells treated with MPP$^+$ (Fig. 3A). Densitometric analysis (Fig. 3B) showed increases in the level of actMMP3 to 232 + 20% and 275 + 25% by 200 μM and 300 μM MPP$^+$, respectively. Under the same conditions, we determined the level of DJ-1 by Western blot analysis using two different antibodies against the C-terminus and N-terminus of DJ-1. The levels of DJ-1 were similarly decreased (11 + 1% and 8 + 1%, respectively; Fig. 3A, middle lanes). Similarly, expressions of both the proMMP3 and actMMP3 were elevated in rotenone-treated CATH.a cells in a dose-dependent manner (Figs. 3C and 3D) and DJ-1 level was also decreased by rotenone treatment. DJ-1 was co-precipitated with MMP3 after MPP$^+$ treatment, confirming physical engagement of the two molecules (Fig. 3E). On the other hand, the level of DJ-1 mRNA was not changed (Figs. 3F and 3G), indicating that the loss of DJ-1 was not a result of transcriptional down-regulation.

Subcellular localization of DJ-1 into the cytosol, mitochondria, and nucleus has been reported (7, 43, 50); thus we tested where MMP3-mediated DJ-1 cleavage occurs. To determine MMP3 and DJ-1 subcellular co-localization, we investigated the localization of DJ-1 and MMP3 after PBS or MPP$^+$ treatment by triple staining of SOD2 for mitochondrial staining, DJ-1, and MMP3. Both MMP3 and DJ-1 were dominantly localized in the cytoplasm with a smaller pool of mitochondrial expression (Fig. 4A). MMP3 level was increased, while DJ-1 expression was largely reduced by MPP$^+$ treatment. Co-localization of DJ-1 and MMP3 was observed in the cytoplasm as well as a minimal extent in the mitochondria (Fig. 4A). To confirm this finding, we investigated the level of proMMP3 and actMMP3 in either the cytosolic and mitochondrial fraction after PBS or MPP$^+$ treatment by Western blot analysis. Although MPP$^+$-induced increase in actMMP3 was only observed in the cytosolic fraction, both the pro- and active form of MMP3 were found in the cytoplasm, as well as mitochondria (Figs. 4B and 4C), suggesting that actMMP3-mediated cleavage of DJ-1 may occur in both subcellular compartments.

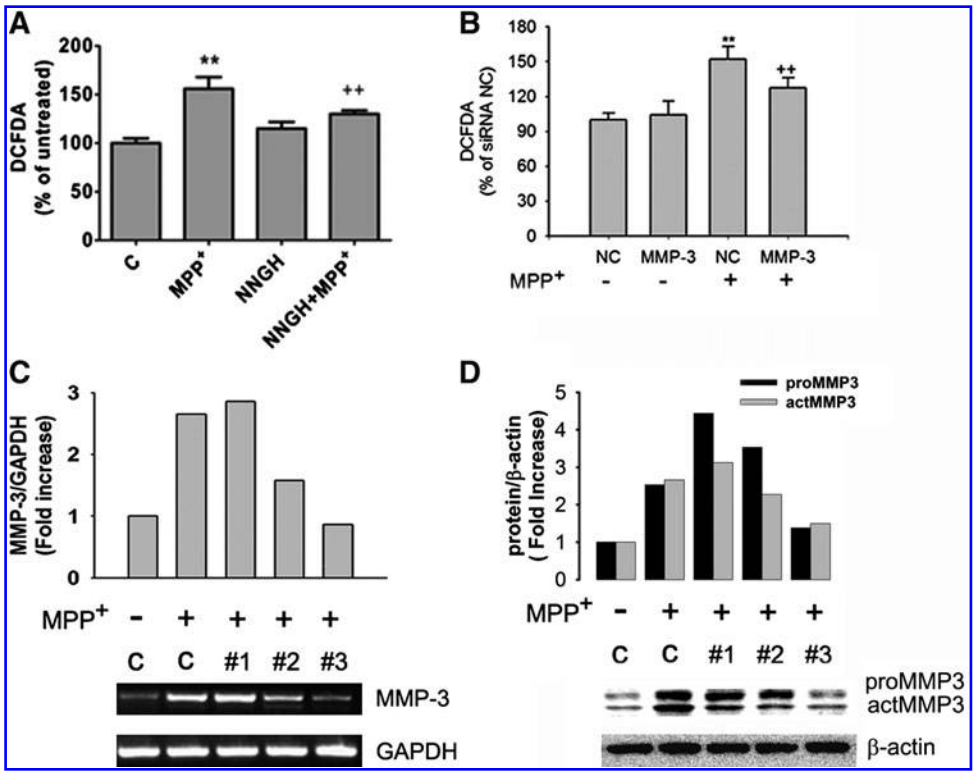

FIG. 2. MMP3 activity is involved in MPP^+-mediated ROS generation. (A) ROS levels were measured using DCFDA in CATH.a cells pretreated with 15 μM NNGH for 1 h, followed by 300 μM MPP^+ for 6 h; $^{**}p < 0.01$ vs. untreated control, $++p < 0.01$ vs. MPP^+ treated. **(B)** ROS levels were measured using DCFDA in cells transfected with MMP3 siRNA. NC, negative control sequence; MMP3, #3 MMP3 siRNA sequence; $^{**}p < 0.01$ vs. NC, $++p < 0.01$ vs. NC + MPP^+ treated. **(C and D)** CATH.a cells were transfected with three different siRNA sequences against MMP3 (#1 ~ #3) and their negative control sequence for 36 h. The cells were then treated with 300 μM MPP^+ for 6 h **(C)** or 24 h **(D).** The knockdown efficiency was verified by RT-PCR **(C)** or Western blot analysis **(D).** GAPDH or β-actin was used as an internal control.

DJ-1 degradation by MMP3 in the substantia nigra of MPTP injected mice

Next, we sought to confirm whether MMP3 is responsible for DJ-1 degradation under toxic stress condition by employing *MMP3* knockout mice treated with MPTP. DJ-1 was expressed in tyrosine hydroxylase (TH)-positive DArgic neurons in the SN (Fig. 5A). Both DJ-1 and TH immunostainings in the SN were significantly decreased at 7 days after MPTP administration as compared to mice treated with vehicle. In *MMP3* null mice, however, decreases in DJ-1 and TH expression caused by MPTP were ameliorated (Fig. 5A). MPTP administration increased both the proMMP3 and actMMP3 protein levels in the SN compared to vehicle-treated wild-type mice in Western blot analysis (Figs. 5B and 5C). Accordingly, both DJ-1 and TH levels were significantly decreased by MPTP treatment. On the other hand, Western blot analysis demonstrated that reduced DJ-1 and TH protein levels were significantly attenuated in *MMP3* null mice treated with MPTP (Figs. 5D and 5E). The results imply that MMP3 plays a role in the degradation of DJ-1 in the SN after MPTP administration.

DJ-1 cleavage and loss of its antioxidant function by cMMP3

Based on these observations, we hypothesized that MMP3 activity might cause cleavage or degradation of DJ-1. In order to detect both N-terminus and C-terminus fragments of DJ-1, full- length human DJ-1 tagged with Flag and V5 on each end was constructed. To test whether MMP3 might directly cleave DJ-1, total protein lysate from COS cells transfected with this construct was incubated with various concentrations (5 to 100 ng/ml) of the catalytic domain of MMP3 (cMMP3) for 2 h, and the resulting fragments were detected by Western blot analysis using either anti-flag or anti-V5 antibody. Both flag-immunopositive N-terminal and V5-immunopositive C-terminal fragments were identified as cMMP3-cleaved peptides (Figs. 6A and 6B). In both cases, about 11-12 kD fragments were identified as a major band with weak large fragments (Figs. 6A and 6B). The fragmentation was effectively attenuated by NNGH (Fig. 6C). The possible cleavage sites of DJ-1, estimated based on molecular sizes of the fragments, appeared to be around amino acids 80 and 110. MMP-9, another member of the MMP family thought to be involved in neurodegeneration (21, 38), had no effect (Fig. 6C), indicating specificity of MMP3 in DJ-1 fragmentation. cMMP3-cleaved DJ-1 fragments were further analyzed by using mass spectrometry. Human recombinant DJ-1 (500 ng) was mixed with cMMP3 (500 ng/ml) for overnight at 37°C (Fig. 6D). Three cleavage sites located between lysine (amino acid 63) and glutamic acid (amino acid 64), between lysine (amino acid 89) and glutamic acid (amino acid 90), and between arginine (amino acid 156) and glycine (amino acid 157) were found (Fig. 6E). The molecular weight of putative each fragment was calculated based on amino acid sequence information, indicating that full-length 3x flag-DJ-1-V5 could be about 24 kD. Western blot analysis, however, showed that the molecular weight of overexpressed protein from the same construct in cells was significantly increased by 3–4 kD, suggesting post-translational modification (Figs. 6A and 6B). Thus, MMP3 cleavage at amino acid 63 and 89 of 3x flag-DJ-1-V5 could generate around 11–12 kD fragments from both ends. This observation, together with mass spectrometry analysis, led us

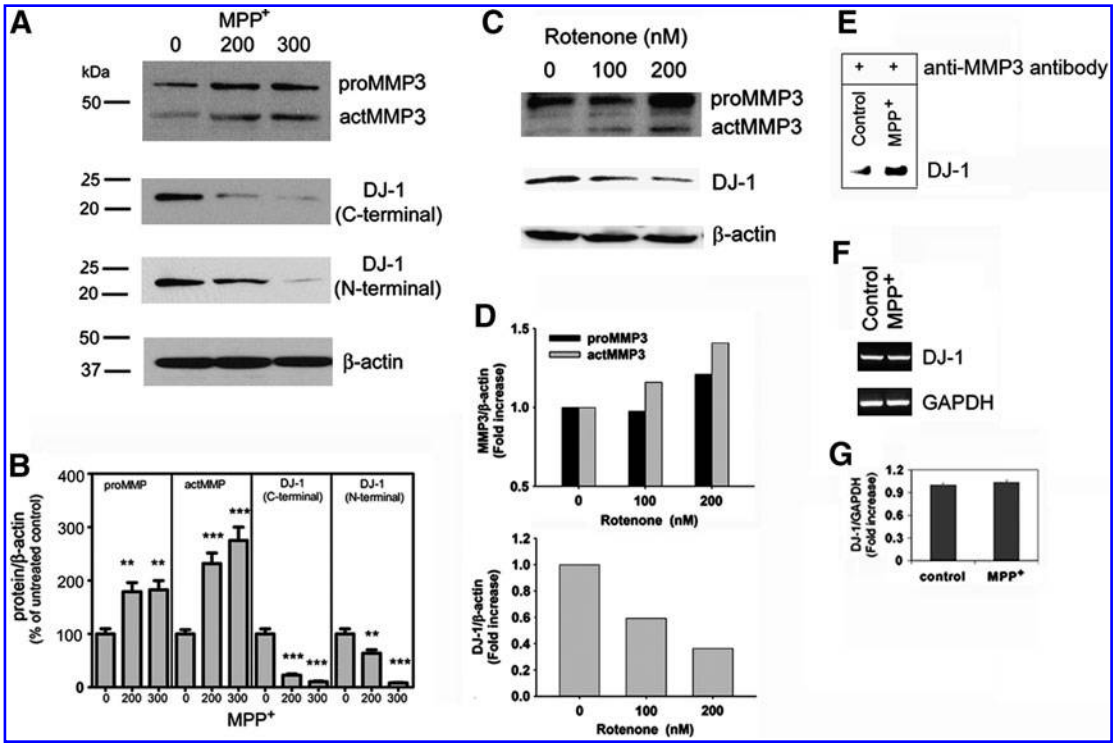

FIG. 3. DJ-1 protein level is decreased without a change in mRNA level in CATH.a cells exposed to MPP^+ or rotenone. **(A)** Representative photomicrographs of Western blot analysis showing MMP3 and DJ-1 levels in CATH.a cells exposed to MPP^+ (200 and 300 μM) for 24 h. (actMMP3, active form of MMP3; c-terminal, antibody against C-terminal epitopes of DJ-1; n-terminal, antibody against N-terminal epitopes of DJ-1; proMMP3, pro-form of MMP3). **(B)** The intensity of each band was determined densitometrically and normalized against β-actin. Expression levels are depicted as percent increase relative to the corresponding untreated control. $^{**}p < 0.01$; $^{***}p < 0.001$ vs. control. **(C)** Representative photomicrographs of Western blot analysis showing MMP3 and DJ-1 levels in CATH.a cells exposed to rotenone (100 and 200 nM) for 24 h. **(D)** The intensity of each band was determined densitometrically and normalized against β-actin. **(E)** Cytosolic fraction of CATH.a cells exposed to MPP^+ was co-immunoprecipitated with anti-MMP3 antibody, then DJ-1 was detected using Western blot analysis. **(F)** A representative PCR of DJ-1 mRNA in CATH.a cells treated with 300 μM MPP^+ for 6 h. **(G)** Real-time PCR confirmed DJ-1 level was not changed by MPP+ treatment. DJ-1 expression level has been normalized against an internal control, GAPDH, and is expressed as fold change of untreated control.

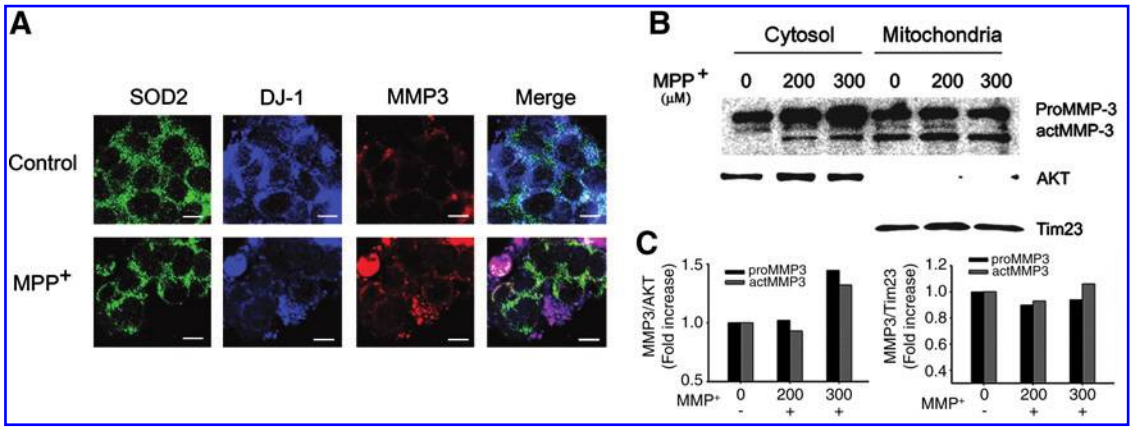

FIG. 4. Subcellular localization of MMP3 and DJ-1 after MPP^+ treatment. **(A)** Representative triple immunofluorescence staining for SOD2 (*green*), MMP3 (*red*), and DJ-1 (*blue*) in CATH.a cells exposed to 300 μM MPP^+ for 24 h (scale, bar = 10 μm), indicating that MMP3 and DJ-1 are co-localized in both cytosol and mitochondria. **(B)** Representative photomicrographs of Western blot analysis showing MMP3 in cytosolic and mitochondrial fraction of CATH.a cells exposed to MPP^+. To determine purity of subcellular fraction, AKT or Tim23 were used as a marker for cytoplasmic or mitochondrial fraction, respectively. **(C)** The intensity of each band was determined densitometrically and normalized against AKT for cytoplasm or Tim23 for mitochondria. (To see this illustration in color the reader is referred to the web version of this article at www.liebertonline.com/ars).

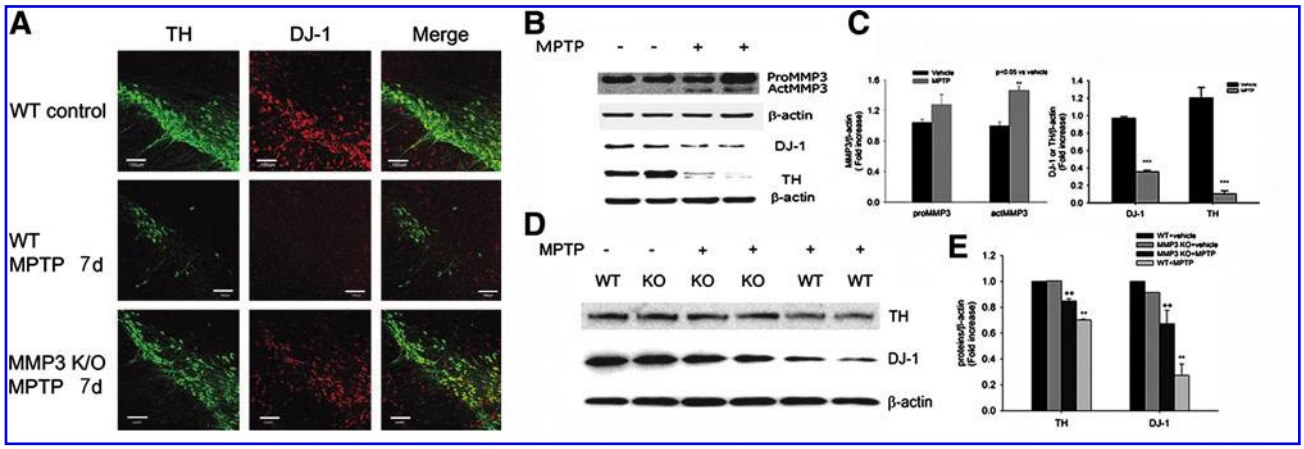

FIG. 5. DJ-1 degradation by MMP3 in the substantia nigra (SN) of mice treated with MPTP. (A) Representative double immunofluorescence staining for tyrosine hydroxylase (TH) (*green*) and DJ-1 (*red*) in SN DA neurons of WT and *MMP-3* null mice after MPTP treatment. Scale bar = 100 μm. WT or *MMP-3* null mice received four intraperitoneal (i.p.) injections of vehicle or MPTP (4×15 mg/kg at 2 h intervals) and were sacrificed after 7 days ($n = 5$ per group). **(B and D)** Western blot analysis showing MMP3, DJ-1, and TH levels in the SN of WT **(B)** or *MMP3* null mice **(D)** injected with MPTP. **(C and E)** The intensity of each band was determined densitometrically and normalized against β-actin. KO, *MMP3* null mice; WT, wild-type mice. $^{**}p < 0.05$; $^{***}p < 0.01$ vs. vehicle or WT + vehicle, $^{++}p < 0.05$ vs. WT+MPTP treated. (To see this illustration in color the reader is referred to the web version of this article at www.liebertonline.com/ars).

to conclude that active MMP3 could preferentially cleave DJ-1 at amino acid 63 and 89 in mixture of flag-DJ-1-V5 transfected cell lysate and cMMP3. As Cys106 of DJ-1 is thought to be responsible for H_2O_2 quenching (3, 7), it is possible that the cleavage around this residue might lead to a loss of the quenching activity. Recombinant full-length human DJ-1 (rDJ-1) was purified from *E. coli* and identified by Coomassie staining (Fig. 6D). rDJ-1 (10 μg/ml) could efficiently quench H_2O_2. This activity was attenuated by the co-incubation with cMMP3 (100 ng/ml), which was restored by the addition of NNGH (Fig. 6F). The results together demonstrated that MMP3 activity is responsible for the fragmentation of DJ-1 and subsequent loss of its H_2O_2 quenching activity.

Fragmentation of DJ-1 in MPP^+-stressed CATH.a cells by actMMP3

We investigated whether the decrease in DJ-1 levels in MPP^+-stressed CATH.a cells is due to cleavage by MMP3. CATH.a cells were transfected with flag-DJ-1-V5 expression cassette followed by MPP^+ treatment. In presence of MPP^+ (300 μM), the 12 kD fragment was generated, detected by both Flag- and V5-antibodies (Figs. 7A and 7B). This peptide was not found in cells cotreated with NNGH (Figs. 7A and 7B). Both DJ-1 monomers and dimers were affected: MMP^+ caused $0.32 + 0.01$- and $0.29 + 0.02$-fold decreases in the monomer and dimer bands, respectively (Figs. 7C and 7D) and both were significantly restored by NNGH to $0.93 + 0.04$- and $0.59 + 0.04$-folds, respectively (Figs. 7C and 7D). The results together suggested that MMP3 was responsible for the DJ-1 fragmentation in MPP^+-stressed CATH.a cells.

Restoration of the DJ-1 protein level by MMP3 knockdown

To further confirm the role of MMP3 on intracellular DJ-1 cleavage, DJ-1 level was measured in CATH.a cells in which MMP3 was selectively blocked by RNAi. Transfection of CATH.a cells with MMP3 siRNA reduced the MPP^+-induced actMMP3 expression from 2.83 ± 0.04-fold (negative control, NC) to 1.48 ± 0.02-fold (Figs. 8A and 8C). In the same condition, DJ-1 level was restored to $99.85 \pm 2.71\%$, compared to the negative control ($61.89 \pm 2.24\%$) (Figs. 8A and 8B).

Attenuation of MPP^+-elicited loss of phosphorylated AKT and cell death by MMP3 inhibition

We tested whether the AKT survival pathway, known to act downstream of DJ-1 (22, 48), may be affected by the MMP3 activity. As shown in Figures 9A and 9B, in the MPP^+-stressed CATH.a cells, the degree of DJ-1 reduction correlated with a decrease in phosphorylated AKT (pAKT) at both Thr308 and Ser473 residues ($43 \pm 4\%$ and $77 \pm 2\%$, respectively). The MMP3 inhibitor NNGH restored the pAKT levels ($75 \pm 4\%$ at Thr308 and $115 \pm 8\%$ at Ser473) along with the DJ-1 level. Of the two sites, the recovery of phosphorylation at Thr308 was more sensitive to and nearly complete with NNGH. Under this condition, cell death was attenuated by NNGH (30 μM) from $205.00 \pm 8.10\%$ to $142.00 \pm 5.80\%$ (Fig. 9C). In addition, MPP^+ treatment of cells transfected with control siRNA (NC) caused $177.39 \pm 15\%$ death, as determined by LDH activity in the medium, and this was significantly reduced in MMP3 siRNA transfected cells ($106.59 \pm 3.4\%$) (Figs. 9D and 9E). Cell death assessed by MTT assay also confirmed this observation (Fig. 9F). All these results demonstrated that inhibition of MMP3 restored pAKT level and attenuated MPP^+-elicited death of CATH.a cells.

Discussion

We demonstrate in the present study that MMP3 is activated under MPP^+-elicited cell stress and cleaves DJ-1, and that this leads to loss of H_2O_2 quenching activity and cell vulnerability to oxidative stress. MMPs are mainly released into the extracellular space as inert proforms and are cleaved to become active forms. Increasing evidence, however, suggests that they could be activated inside cells, cleave cytosolic targets, and modulate cellular functions (28). MMP3 also

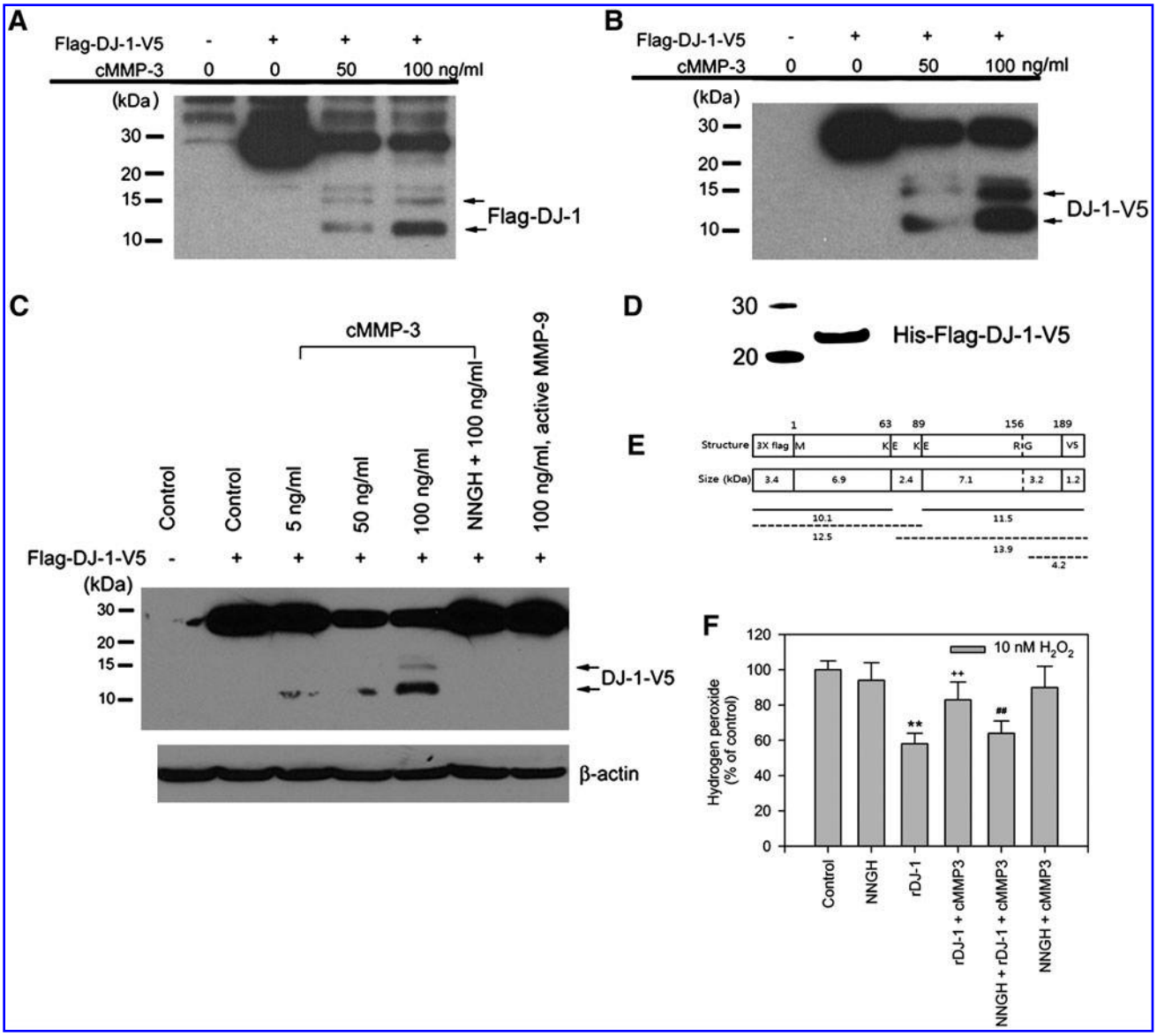

FIG. 6. DJ-1 fragmentation by MMP3 results in a loss of its H_2O_2 quenching activity. (A, B, and C) Representative photomicrographs of Western blots performed against Flag (N-terminus tag, **A**) and V5 (C-terminus tag, **B**) in total lysates of COS cells overexpressing Flag-DJ-1-V5 after 2 h incubation with cMMP3 (5 ng/ml, 50 ng/ml, and 100 ng/ml) in the absence or presence NNGH or MMP9 **(C).** Two Flag-immunopositive N-terminal fragments of 12 (*lower arrow*) and 15 (*upper arrow*) kD **(A)** and two V5-immunopositive C-terminal fragments of 12 (*lower arrow*) and 15 (*upper arrow*) kD **(B and C)** were identified. **(D)** Preparation of recombinant DJ-1 tagged with Flag (N-terminus) and V5 (C-terminus) (rDJ-1). A recombinant full-length human DJ-1 tagged with Flag or V5 at its N- and C-terminus, respectively, was purified from *E. coli* and was identified by Coomassie blue after SDS-PAGE. **(E)** Schematic diagram of putative cleavage sites and expected molecular weight (kD) of recombinant flag-DJ-1-v5 fragments by cMMP3 analyzed using mass spectrometry. *Lower panel* depicts putative fragments and their molecular weight. While *solid lines* indicate main peptide fragments expected after cMMP3 cleavage, *dotted lines* represent minor fragments. **(F)** DJ-1 H_2O_2 quenching activity following incubation of 10 μg/ml of recombinant DJ-1 with 100 ng/ml of cMMP3 in the absence or presence of NNGH for 2 h. $^{**}p < 0.01$ vs. control, $++p < 0.01$ vs. rDJ-1 incubation, ##p < 0.01 vs. rDJ-1 and cMMP-3 incubation.

localizes into various subcellular compartments, including nucleus and cytoplasm (8, 39). Previously, we found that MMP3 could be activated intracellularly in DArgic cells upon oxidative stress and is involved in apoptosis (8). Here, we found that both the pro- and active form of MMP3 are in the cytosol and mitochondria. DJ-1, a member of hydroperoxide responsive proteins (29), is an atypical peroxiredoxins-like peroxidase that scavenges mitochondrial H_2O_2 (3). Human DJ-1 consists of 189 amino acids (22 kD) and may undergo conformational changes to acquire catalytic activity in response to oxidative stress. It has been reported that the alpha-helix at the C-terminal region appears to regulate the enzymatic activity (14), and Cys-106, His-126, and Glu-18 may be important residues in the catalytic site of DJ-1 (44). A recent publication positively confirmed the previous results obtained from cellular models (7, 24, 29) that oxidative

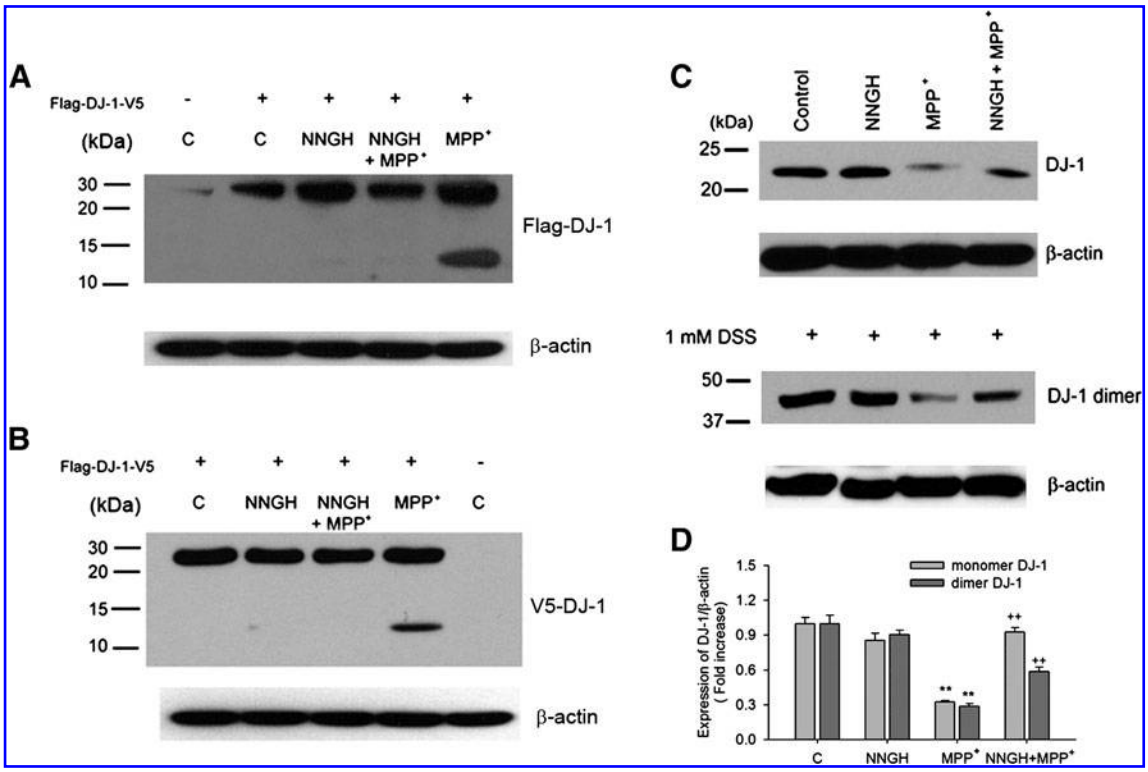

FIG. 7. DJ-1 degradation is reduced by MMP3 inhibition. (A and B) Representative photomicrographs of Western blots performed against Flag (N-terminus tag, **A**) and V5 (C-terminus tag, **B**). CATH.a cells were transiently transfected with DJ-1 plasmid DNA tagged with Flag and V5 for 36 h and then treated with 300 μM of MPP^+ in the presence or absence of NNGH. **(C)** DJ-1 protein levels (monomer and dimer) were detected by Western blot analysis. To determine of endogenous dimer DJ-1, 1 mM DSS (cross-linker) was added to the CATH.a cell lysate. **(D)** DJ-1 protein levels determined by densitometric analysis were expressed as fold changes of untreated control. $^{**}p < 0.01$ vs. untreated control, $++p < 0.01$ vs. MPP^+ treated.

conditions induce the formation of sulfinic acid ($-SO_2H$) at Cys-106 (3). These findings led to the conclusion that both the Cys-106 and C-terminal region are required for DJ-1 to respond to and protect cells against oxidative stress. Therefore, removing these sites would be expected to result in loss of the quenching activity. The present finding shows that MMP3 leads to disruption of the DJ-1 catalytic activity by causing fragmentation. Mass spectrometry analysis suggested putative three cleavage sites for MMP3 in DJ-1 at amino acid numbers 63, 89, or 156, resulting in DJ-1 fragmentation. Our result suggests that MMP3 preferentially cleaves amino acid 63 and 89 inside cells under stress condition. This fragmentation could impair DJ-1 function and lead to decrease H_2O_2 quenching activity in oxidative stressed condition. The sizes

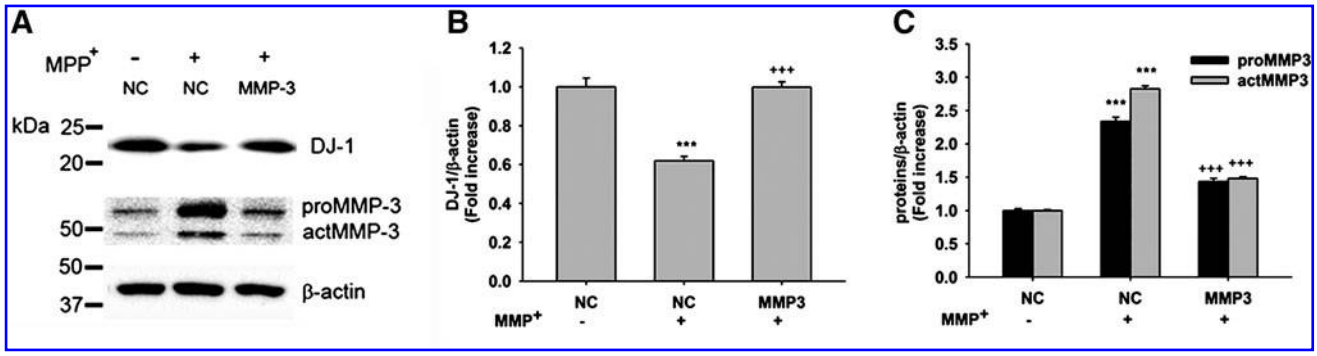

FIG. 8. MPP^+-induced DJ-1 degradation is recovered by MMP3 knockdown. (A) Representative photomicrographs of Western blots performed against DJ-1, proMMP3, and actMMP3. Cells were transfected with negative control siRNA (NC) or mouse MMP3 siRNA (MMP3) for 36 h and then treated with 300 μM of MPP^+. β-actin was used as an internal control. **(B and C)** DJ-1 or actMMP3 levels were quantified using densitometric analysis and normalized against β-actin. $^{***}p < 0.01$ vs. NC and $+++p < 0.01$ vs. NC + MPP^+.

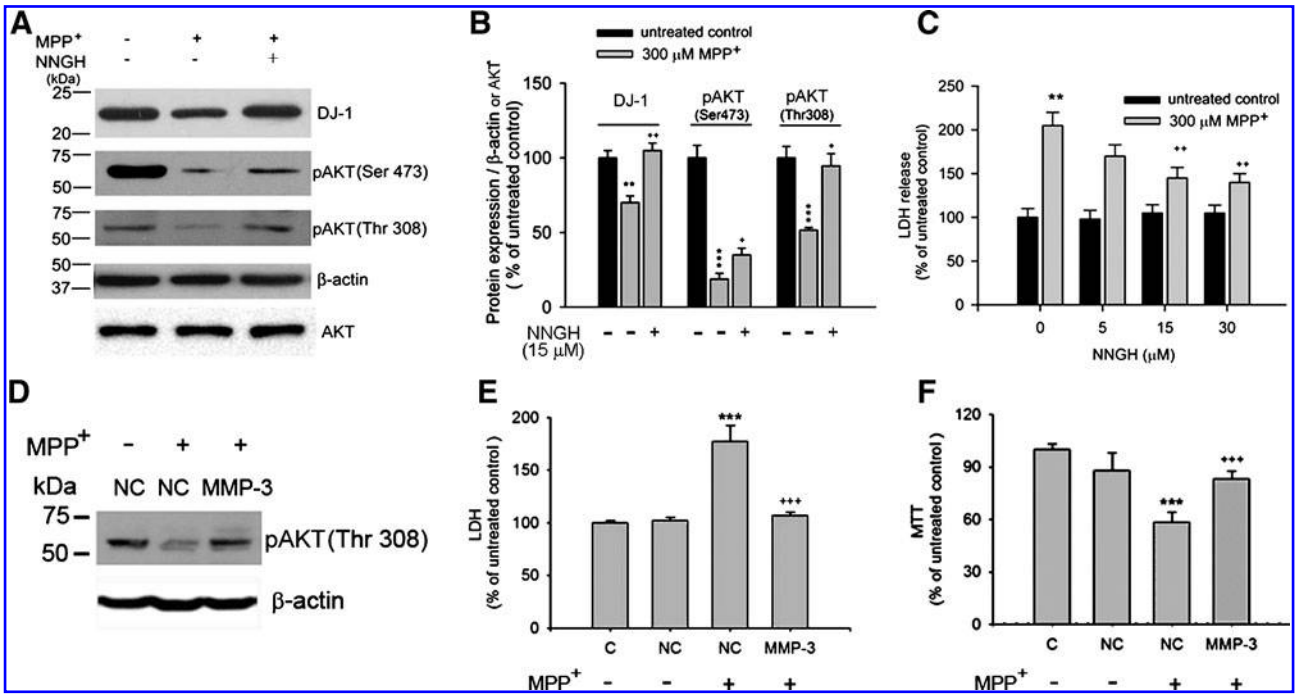

FIG. 9. MPP$^+$-mediated cell death and reduced Akt phosphorylation are inhibited by MMP3 inhibition. (A) Representative photomicrographs of Western blots performed against DJ-1, pAKT (Ser473) and pAKT (Thr308) in MPP$^+$-stressed CATH.a cells in the presence or absence of NNGH. DJ-1 or pAKTs levels were quantified using densitometric analysis and normalized against β-actin or AKT, respectively. **(B)** DJ-1 and phospho-AKT levels were determined by densitometric analysis and expressed as % of untreated control. $^{**}p < 0.01$; $^{***}p < 0.001$ vs. respective untreated control; $+p < 0.05$; $++p < 0.01$ vs MPP$^+$ alone. **(C)** Cell death was assessed by LDH activity released in the media of CATH.a cells treated with various concentrations of NNGH (5, 15, and 30 μM) for 1 h, followed by 300 μM MPP$^+$. $^{**}p < 0.01$ vs. untreated control; $++p < 0.05$ vs. MPP$^+$ alone. **(D)** Representative photomicrographs of Western blots performed against pAkt (Thr308). Cells were transfected with negative control siRNA (NC) or mouse MMP3 siRNA (MMP3) for 36 h and then treated with 300 μM of MPP$^+$. Cell death was assessed by LDH activity in the medium **(E)** and MTT reduction **(F).** $^{***}p < 0.001$ vs. negative control (NC) and $+++p < 0.001$ vs. NC + MPP$^+$.

of fragmented DJ-1 were similar to ones detected in MPP$^+$-treated cells by Western blot. It was reported that direct oxidative insult such as H_2O_2 to DJ-1 leads to cleavage between glycine and proline at amino acid numbers 157 and 158, respectively (34). Further investigation of postmortem PD brain tissue might be necessary to confirm whether DJ-1 fragmentation occurs in human PD patients. It has been demonstrated that MMP9, another member of the MMP family, is involved in the neuronal damage following ischemia (16). Because NNGH can inhibit MMP9 as well, one cannot completely eliminate the possibility that MMP9 may also be involved. However, the present study showed that catalytically active MMP9 did not cleave DJ-1 *in vitro*. In addition, we have previously observed that MMP9 is not altered in response to cell stress in CATH.a cells (8). Together with the results that siRNA-mediated specific MMP3 knockdown also reduced DJ-1 degradation, MMP3 seems to be the major protease that cleaves DJ-1 in DArgic cells under cell stress.

Analysis of the crystal structure of DJ-1 has revealed that it may function as a dimer (13, 14, 16, 47), and the loss of function caused by the PD-associated mutations, Leu-166-Pro and Arg-28-Ala, is due to either destabilization of the dimer interface or conformational changes (13, 47). The dimerization is thought to require intact Leu-166, since the Leu-166-Pro mutant exhibited impaired ability to self-interact to form homo-oligomers (31). The fragmentation by MMP3 would interrupt with the dimerization process. Indeed, we observed that cMMP3 treatment decreased DJ-1 dimer. Therefore, it seems that the MMP3 causes a loss of DJ-1 activity by removing regions that are critical for catalytic activity and dimerization.

MPP$^+$, a toxic metabolite of MPTP, is an inhibitor of complex I of the mitochondrial electron transfer chain, which leads to generation of ROS (2a, 47a). Selective MMP3 inhibition by either NNGH or MMP3 siRNA reduced MPP$^+$-induced ROS level as well as DJ-1degradation, suggesting MMP3 may increase ROS level by DJ-1 degradation. Previously, we reported that MPTP-mediated DArgic neuronal degeneration was largely attenuated in *MMP3* null mice (23). *In vivo* experiment using *MMP3* null mice treated with MPTP further confirmed that MMP3 is responsible for reduced DJ-1 protein level and DArgic neuronal degeneration in the SN. Activation of MMPs in neurodegenerative conditions was reported. S-nitrosylation-mediated MMP9 activation was observed in cerebral ischemia and involved in neuronal cell death (12, 42) It has also been demonstrated that ROS leads to expression of MMP3 (46). Taken together, it is possible to envision a vicious cycle between oxidative stress, MMP3, and DJ-1 cleavage. Stress conditions leading to intracellular oxidative stress could cause induction and activation of MMP3. Next, fragmentation of DJ-1 by MMP3 could abolish DJ-1's ROS quenching activity,

leading to further accumulation of ROS and further induction of MMP3.

Previous studies have shown that DJ-1 modulates the PTEN/AKT survival pathway (22, 48). DJ-1 overexpression leads to hyperphosphorylation of PKB/AKT and increased cell survival (22). In the present study, AKT phosphorylated at Thr308 and Ser473 were downregulated by MPP^+, and this was restored in the presence of NNGH. The restoration appeared more effective at Thr308, which was restored nearly to the control (no MPP^+) levels in the presence of 15 μM NNGH. The results raise an interesting question. It is thought that Thr308 in the membrane-bound AKT is preferentially phosphorylated by activated phosphoinositide-dependent kinase 1 (PDK1) (1, 10, 20), whereas Ser473 is likely phosphorylated by integrin-linked kinase (ILK) (35, 49). Since the MPP^+-elicited downregulation of pAKT(Thr308) was more effectively restored than pAKT(Ser473) by NNGH, the mechanism underlying the pAKT downregulation may be due to reduction in PI3K-activated PDK activity. In addition, recent studies have linked DJ-1 to the PI3K/AKT survival pathway through its suppression of phosphatase and tensin homolog deleted on chromosome ten (PTEN, (22, 48)), and downregulation of AKT is thought to promote cell death through either BAD/Bcl-XL complex or inactivation of IKK-α and NF-κB (32). Thus, the cleavage of DJ-1 by MMP3 may reverse this suppressive effect. It is hard to exclude, however, other possibility that MMP3 could affect on AKT pathway through other mechanisms such as target molecular shedding on DArgic neuronal surface.

In summary, the present study demonstrates that actMMP3 in stressed CATH.a cells cleaves DJ-1, and the cleavage results in loss of a protective role of DJ-1 against oxidative cell damage. The study also suggests the possibility that actMMP3 may serve as a target for pharmacological intervention of PD.

Acknowledgments

We thank Dr. Tong H. Joh for his various advices on experiments as well as writing of this manuscript. This research was supported by Parkinson's Disease Foundation (Dong-Hee Choi, FY 2006-2007), and Brain Research Center of the 21st Century Frontier Research Program (2010K000810) of the Ministry of Education, Science and Technology, the Republic of Korea, to O. Hwang.

Author Disclosure Statement

The authors declare that they have no competing financial interests.

References

1. Alessi DR, Kozlowski MT, Weng QP, Morrice N, and Avruch J. 3-Phosphoinositide-dependent protein kinase 1 (PDK1) phosphorylates and activates the p70 S6 kinase *in vivo* and *in vitro*. *Curr Biol* 8: 69–81, 1998.
2. Aleyasin H, Rousseaux MW, Phillips M, Kim RH, Bland RJ, Callaghan S, Slack RS, During MJ, Mak TW, and Park DS. The Parkinson's disease gene DJ-1 is also a key regulator of stroke-induced damage. *Proc Natl Acad Sci USA* 104: 18748–18753, 2007.

2a. Anantharam V, Kaul S, Song C, Kanthasamy A, and Kanthasamy AG. Pharmacological inhibition of neuronal NADPH oxidase protects against 1-methyl-4-phenylpyridinium (MPP+)-induced oxidative stress and apoptosis in mesencephalic dopaminergic neuronal cells. *Neurotoxicology* 28: 988–997, 2007.

3. Andres–Mateos E, Perier C, Zhang L, Blanchard–Fillion B, Greco TM, Thomas B, Ko HS, Sasaki M, Ischiropoulos H, Przedborski S, Dawson TM, and Dawson VL. DJ-1 gene deletion reveals that DJ-1 is an atypical peroxiredoxin-like peroxidase. *Proc Natl Acad Sci USA* 104: 14807–14812, 2007.
4. Bader V, Ran Zhu X, Lubbert H, and Stichel CC. Expression of DJ-1 in the adult mouse CNS. *Brain Res* 1041: 102–111, 2005.
5. Bandopadhyay R, Kingsbury AE, Cookson MR, Reid AR, Evans IM, Hope AD, Pittman AM, Lashley T, Canet–Aviles R, Miller DW, McLendon C, Strand C, Leonard AJ, Abou–Sleiman PM, Healy DG, Ariga H, Wood NW, de Silva R, Revesz T, Hardy JA, and Lees AJ. The expression of DJ-1 (PARK7) in normal human CNS and idiopathic Parkinson's disease. *Brain* 127: 420–430, 2004.
6. Bonifati V, Rizzu P, van Baren MJ, Schaap O, Breedveld GJ, Krieger E, Dekker MC, Squitieri F, Ibanez P, Joosse M, van Dongen JW, Vanacore N, van Swieten JC, Brice A, Meco G, van Duijn CM, Oostra BA, and Heutink P. Mutations in the DJ-1 gene associated with autosomal recessive early-onset parkinsonism. *Science* 299: 256–259, 2003.
7. Canet–Aviles RM, Wilson MA, Miller DW, Ahmad R, McLendon C, Bandyopadhyay S, Baptista MJ, Ringe D, Petsko GA, and Cookson MR. The Parkinson's disease protein DJ-1 is neuroprotective due to cysteine-sulfinic acid-driven mitochondrial localization. *Proc Natl Acad Sci USA* 101: 9103–9108, 2004.
8. Choi DH, Kim EM, Son HJ, Joh TH, Kim YS, Kim D, Flint Beal M, and Hwang O. A novel intracellular role of matrix metalloproteinase-3 during apoptosis of dopaminergic cells. *J Neurochem* 106: 405–415, 2008.
9. Choi J, Sullards MC, Olzmann JA, Rees HD, Weintraub ST, Bostwick DE, Gearing M, Levey AI, Chin LS, and Li L. Oxidative damage of DJ-1 is linked to sporadic Parkinson and Alzheimer diseases. *J Biol Chem* 281: 10816–10824, 2006.
10. Delcommenne M, Tan C, Gray V, Rue L, Woodgett J, and Dedhar S. Phosphoinositide-3-OH kinase-dependent regulation of glycogen synthase kinase 3 and protein kinase B/AKT by the integrin-linked kinase. *Proc Natl Acad Sci USA* 95: 11211–11216, 1998.
11. Faust K, Gehrke S, Yang Y, Yang L, Beal F, and Lu B. Neuroprotective effects of compounds with antioxidant and anti-inflammatory properties in a Drosophila model of Parkinson's disease. *BMC Neurosci* 10: 109, 2009.
12. Gu Z, Kaul M, Yan B, Kridel SJ, Cui J, Strongin A, Smith JW, Liddington RC, and Lipton SA. S-nitrosylation of matrix metalloproteinases: Signaling pathway to neuronal cell death. *Science* 297: 1186–1190, 2002.
13. Herrera FE, Zucchelli S, Jezierska A, Lavina ZS, Gustincich S, and Carloni P. On the oligomeric state of DJ-1 protein and its mutants associated with Parkinson Disease. A combined computational and *in vitro* study. *J Biol Chem* 282: 24905–24914, 2007.
14. Honbou K, Suzuki NN, Horiuchi M, Niki T, Taira T, Ariga H, and Inagaki F. The crystal structure of DJ-1, a protein related to male fertility and Parkinson's disease. *J Biol Chem* 278: 31380–31384, 2003.
15. Horstmann S, Kalb P, Koziol J, Gardner H, and Wagner S. Profiles of matrix metalloproteinases, their inhibitors, and laminin in stroke patients: Influence of different therapies. *Stroke* 34: 2165–2170, 2003.
16. Huai Q, Sun Y, Wang H, Chin LS, Li L, Robinson H, and Ke H. Crystal structure of DJ-1/RS and implication on familial Parkinson's disease. *FEBS Lett* 549: 171–175, 2003.

17. Ishikawa S, Taira T, Niki T, Takahashi–Niki K, Maita C, Maita H, Ariga H, and Iguchi–Ariga SM. Oxidative status of DJ-1-dependent activation of dopamine synthesis through interaction of tyrosine hydroxylase and L-DOPA decarboxylase with DJ-1. *J Biol Chem* 284: 28832–28844, 2009.
18. This reference has been deleted.
19. Junn E, Taniguchi H, Jeong BS, Zhao X, Ichijo H, and Mouradian MM. Interaction of DJ-1 with Daxx inhibits apoptosis signal-regulating kinase 1 activity and cell death. *Proc Natl Acad Sci US A* 102: 9691–9696, 2005.
20. Kandel ES and Hay N. The regulation and activities of the multifunctional serine/threonine kinase Akt/PKB. *Exp Cell Res* 253: 210–229, 1999.
21. Kim GW, Gasche Y, Grzeschik S, Copin JC, Maier CM, and Chan PH. Neurodegeneration in striatum induced by the mitochondrial toxin 3-nitropropionic acid: Role of matrix metalloproteinase-9 in early blood-brain barrier disruption? *J Neurosci* 23: 8733–8742, 2003.
22. Kim RH, Peters M, Jang Y, Shi W, Pintilie M, Fletcher GC, DeLuca C, Liepa J, Zhou L, Snow B, Binari RC, Manoukian AS, Bray MR, Liu FF, Tsao MS, and Mak TW. DJ-1, a novel regulator of the tumor suppressor PTEN. *Cancer Cell* 7: 263–273, 2005.
23. Kim YS, Choi DH, Block ML, Lorenzl S, Yang L, Kim YJ, Sugama S, Cho BP, Hwang O, Browne SE, Kim SY, Hong JS, Beal MF, and Joh TH. A pivotal role of matrix metalloproteinase-3 activity in dopaminergic neuronal degeneration via microglial activation. *FASEB J* 21: 179–187, 2007.
24. Kinumi T, Kimata J, Taira T, Ariga H, and Niki E. Cysteine-106 of DJ-1 is the most sensitive cysteine residue to hydrogen peroxide-mediated oxidation *in vivo* in human umbilical vein endothelial cells. *Biochem Biophys Res Commun* 317: 722–728, 2004.
25. Kumaran R, Vandrovcova J, Luk C, Sharma S, Renton A, Wood NW, Hardy JA, Lees AJ, and Bandopadhyay R. Differential DJ-1 gene expression in Parkinson's disease. *Neurobiol Dis* 36: 393–400, 2009.
26. Levin J, Giese A, Boetzel K, Israel L, Hogen T, Nubling G, Kretzschmar H, and Lorenzl S. Increased alpha-synuclein aggregation following limited cleavage by certain matrix metalloproteinases. *Exp Neurol* 215: 201–208, 2009.
27. Livak KJ ST. Analysis of relative gene expression data using real-time quantitative PCR and the 2(-Delta Delta C(T)) method. *Methods* 25: 402–408, 2001.
28. Miller JP, Holcomb J, Al–Ramahi I, de Haro M, Gafni J, Zhang N, Kim E, Sanhueza M, Torcassi C, Kwak S, Botas J, Hughes RE, and Ellerby LM. Matrix metalloproteinases are modifiers of huntingtin proteolysis and toxicity in Huntington's disease. *Neuron* 67: 199–212, 2010.
29. Mitsumoto A, Nakagawa Y, Takeuchi A, Okawa K, Iwamatsu A, and Takanezawa Y. Oxidized forms of peroxiredoxins and DJ-1 on two-dimensional gels increased in response to sublethal levels of paraquat. *Free Radic Res* 35: 301–310, 2001.
30. Miyazaki I, Asanuma M, Diaz–Corrales FJ, Fukuda M, Kitaichi K, Miyoshi K, and Ogawa N. Methamphetamine-induced dopaminergic neurotoxicity is regulated by quinone-formation-related molecules. *FASEB J* 20: 571–573, 2006.
31. Moore DJ, Zhang L, Dawson TM, and Dawson VL. A missense mutation (L166P) in DJ-1, linked to familial Parkinson's disease, confers reduced protein stability and impairs homo-oligomerization. *J Neurochem* 87: 1558–1567, 2003.
32. Mortenson MM, Galante JG, Gilad O, Schlieman MG, Virudachalam S, Kung HJ, and Bold RJ. BCL-2 functions as an activator of the AKT signaling pathway in pancreatic cancer. *J Cell Biochem* 102: 1171–1179, 2007.
33. Nagakubo D, Taira T, Kitaura H, Ikeda M, Tamai K, Iguchi–Ariga SM, and Ariga H. DJ-1, a novel oncogene which transforms mouse NIH3T3 cells in cooperation with ras. *Biochem Biophys Res Commun* 231: 509–513, 1997.
34. Ooe H, Maita C, Maita H, Iguchi–Ariga SM, and Ariga H. Specific cleavage of DJ-1 under an oxidative condition. *Neurosci Lett* 406: 165–168, 2006.
35. Persad S, Attwell S, Gray V, Mawji N, Deng JT, Leung D, Yan J, Sanghera J, Walsh MP, and Dedhar S. Regulation of protein kinase B/Akt-serine 473 phosphorylation by integrin-linked kinase: Critical roles for kinase activity and amino acids arginine 211 and serine 343. *J Biol Chem* 276: 27462–27469, 2001.
36. Qu W, Fan L, Kim YC, Ishikawa S, Iguchi–Ariga SM, Pu XP, and Ariga H. Kaempferol derivatives prevent oxidative stress-induced cell death in a DJ-1-dependent manner. *J Pharmacol Sci* 110: 191–200, 2009.
37. Ramsey CP and Giasson BI. The E163K DJ-1 mutant shows specific antioxidant deficiency. *Brain Res* 1239: 1–11, 2008.
38. Romanic AM, White RF, Arleth AJ, Ohlstein EH, and Barone FC. Matrix metalloproteinase expression increases after cerebral focal ischemia in rats: Inhibition of matrix metalloproteinase-9 reduces infarct size. *Stroke* 29: 1020–1030, 1998.
39. Si–Tayeb K MA, Mazzocco C, Lepreux S, Decossas M, Cubel G, Taras D, Blanc JF, Robinson DR, Rosenbaum J. Matrix metalloproteinase 3 is present in the cell nucleus and is involved in apoptosis. *Am J Pathol* 169: 1390, 2006.
40. Sung JY, Park SM, Lee CH, Um JW, Lee HJ, Kim J, Oh YJ, Lee ST, Paik SR, and Chung KC. Proteolytic cleavage of extracellular secreted {alpha}-synuclein via matrix metalloproteinases. *J Biol Chem* 280: 25216–25224, 2005.
41. Suri C, Fung BP, Tischler AS, and Chikaraishi DM. Catecholaminergic cell lines from the brain and adrenal glands of tyrosine hydroxylase-SV40 T antigen transgenic mice. *J Neurosci* 13: 1280–1291, 1993.
42. Svineng G, Ravuri C, Rikardsen O, Huseby NE, and Winberg JO. The role of reactive oxygen species in integrin and matrix metalloproteinase expression and function. *Connect Tissue Res* 49: 197–202, 2008.
43. Taira T, Saito Y, Niki T, Iguchi–Ariga SM, Takahashi K, and Ariga H. DJ-1 has a role in antioxidative stress to prevent cell death. *EMBO Rep* 5: 213–218, 2004.
44. Tao X and Tong L. Crystal structure of human DJ-1, a protein associated with early onset Parkinson's disease. *J Biol Chem* 278: 31372–31379, 2003.
45. This reference has been deleted.
46. Ward SK, Wakamatsu TH, Dogru M, Ibrahim OM, Kaido M, Ogawa Y, Matsumoto Y, Igarashi A, Ishida R, Shimazaki J, Schnider C, Negishi K, Katakami C, and Tsubota K. The role of oxidative stress and inflammation in conjunctivochalasis. *Invest Ophthalmol Vis Sci* 51: 1994–2002, 2010.
47. Wilson MA, Collins JL, Hod Y, Ringe D, and Petsko GA. The 1.1-A resolution crystal structure of DJ-1, the protein mutated in autosomal recessive early onset Parkinson's disease. *Proc Natl Acad Sci USA* 100: 9256–9261, 2003.
47a. Xie J, Duan L, Qian X, Huang X, Ding J, and Hu G. KATP channel openers protect mesencephalic neurons against MPP+-induced cytotoxicity via inhibition of ROS production. *J Neurosci Res* 88: 428–437, 2010.
48. Yang Y, Gehrke S, Haque ME, Imai Y, Kosek J, Yang L, Beal MF, Nishimura I, Wakamatsu K, Ito S, Takahashi R, and Lu B. Inactivation of Drosophila DJ-1 leads to impairments

of oxidative stress response and phosphatidylinositol 3-kinase/Akt signaling. *Proc Natl Acad Sci USA* 102: 13670–13675, 2005.
49. Yoganathan TN, Costello P, Chen X, Jabali M, Yan J, Leung D, Zhang Z, Yee A, Dedhar S, and Sanghera J. Integrin-linked kinase (ILK): a "hot" therapeutic target. *Biochem Pharmacol* 60: 1115–1119, 2000.
50. Zhang L, Shimoji M, Thomas B, Moore DJ, Yu SW, Marupudi NI, Torp R, Torgner IA, Ottersen OP, Dawson TM, and Dawson VL. Mitochondrial localization of the Parkinson's disease related protein DJ-1: Implications for pathogenesis. *Hum Mol Genet* 14: 2063–2073, 2005.

Address correspondence to:
Dr. Yoon-Seong Kim
Department of Neurology/Neuroscience, A578
Weill Medical College of Cornell University
525 East 68th Street
New York, NY 10065

E-mail: yok2001@med.cornell.edu

Date of first submission to ARS Central, December 15, 2009; date of final revised submission, October 12, 2010; date of acceptance, October 24, 2010.

Abbreviations Used

actMMP = active form of matrix metalloproteinases
cMMP = catalytic domain of matrix metalloproteinases
CNS = central nervous system
DA = dopamine
DCFDA = 2′,7′-dichlorodihydrofluorescein diacetate
DMSO = dimethyl sulfoxide
GAPDH = glyceraldehyde 3-phosphate dehydrogenase
IKK-α = I kappa B kinase
IPTG = isopropyl β-thiogalactopyranoside
JNK = Jun N-terminal kinase
LDH = lactate dehydrogenase
MPP^+ = 1-methyl-4-phenylpyridinium
MPTP = 1-methyl-4-phenyl-1,2,3,6-tetrahydropyridine
MTT = 3-(4,5-dimethylthiazal-2-yl)-2,5-diphenyl-tetrazolium bromide
NF-κB = nuclear factor kappa-B
NNGH = N-isobutyl-N-(4-methoxyphenylsulfonyl) glycyl hydroxamic acid
PD = Parkinson's disease
PI3K = phosphatidylinositol 3-kinase
ROS = reactive oxygen species
SNpc = substantia nigra pars compacta
SOD2 = superoxide dismutase 2, mitochondrial manganese superoxide dismutase 2

This article has been cited by:

1. Inge Van Hove, Kim Lemmens, Sarah Van de Velde, Mieke Verslegers, Lieve Moons. 2012. Matrix metalloproteinase-3 in the central nervous system: a look on the bright side. *Journal of Neurochemistry* **123**:2, 203-216. [CrossRef]
2. Maria Xilouri, Oystein Rod Brekk, Leonidas Stefanis. 2012. Alpha-synuclein and Protein Degradation Systems: a Reciprocal Relationship. *Molecular Neurobiology* . [CrossRef]
3. Katrin Beyer, Aurelio Ariza. 2012. Alpha-Synuclein Posttranslational Modification and Alternative Splicing as a Trigger for Neurodegeneration. *Molecular Neurobiology* . [CrossRef]
4. G Robert, A Puissant, M Dufies, S Marchetti, A Jacquel, T Cluzeau, P Colosetti, N Belhacene, P Kahle, C A Da Costa, F Luciano, F Checler, P Auberger. 2012. The caspase 6 derived N-terminal fragment of DJ-1 promotes apoptosis via increased ROS production. *Cell Death and Differentiation* . [CrossRef]
5. Yoon-Seong Kim, Tong-H. Joh. 2012. Matrix Metalloproteinases, New Insights into the Understanding of Neurodegenerative Disorders. *Biomolecules and Therapeutics* **20**:2, 133-143. [CrossRef]
6. Eun Jung Shin, Eun-Mee Kim, Ji Ae Lee, Hyangshuk Rhim, Onyou Hwang. 2012. Matrix metalloproteinase-3 is activated by HtrA2/Omi in dopaminergic cells: Relevance to Parkinson's disease. *Neurochemistry International* . [CrossRef]
7. Ana Rita Vaz, Sandra L. Silva, Andreia Barateiro, Ana Sofia Falcão, Adelaide Fernandes, Maria A. Brito, Dora Brites. 2011. Selective vulnerability of rat brain regions to unconjugated bilirubin. *Molecular and Cellular Neuroscience* **48**:1, 82-93. [CrossRef]
8. Jino Son, Sung-Eun Lee, Byeoung-Soo Park, Jinho Jung, Hyung Soon Park, Joo Young Bang, Gum-Yong Kang, Kijong Cho. 2011. Biomarker discovery and proteomic evaluation of cadmium toxicity on a collembolan species, Paronychiurus kimi (Lee). *PROTEOMICS* **11**:11, 2294-2307. [CrossRef]